

## MEASUREMENTS OF $^{232}\text{Th}/^{238}\text{U}$ RATIO USING DIFFERENT TECHNIQUES: A COMPARATIVE STUDY

W. Arafa<sup>1</sup>, H. M. Mahmoud<sup>1</sup>, E. Yousf<sup>2</sup>, A. Ashry<sup>3</sup>, A. Elersy<sup>4</sup>, I. Elaassy<sup>2</sup>, H. El Samman<sup>5\*</sup>

<sup>1</sup>Faculty of Women, Ain Shams University, Cairo, Egypt

<sup>2</sup>Nuclear Material Authority, Cairo, Egypt

<sup>3</sup>Faculty of Education, Ain Shams University, Cairo, Egypt

<sup>4</sup>National Institute of Standard, Giza, Egypt

<sup>5</sup>Menoufia University, Shibin Al Koom, Egypt

**Abstract.** The present work was conducted to determine Th/U ratios in different types of natural rock samples (sedimentary, conglomerate, igneous and sediments) using high-purity germanium detector, solid state nuclear track detectors and inductively coupled plasma mass spectrometers. A thin source approach method for alpha tracks measurements was used. A new method was introduced for forming a thin layer of the rock sample. The track densities were obtained using an optical microscope coupled with a digital camera and spark counter. Even though the measurements were carried out using very different techniques, they showed comparable values of Th/U ratio for most of the rock samples.

**Keywords:** CR-39, Gamma spectrometer, LR-115-II, (ICP-MS), Th/U ratio

### 1. INTRODUCTION

Primordial radionuclides are as old as the Earth. The most significant of these are the radionuclides of the  $^{238}\text{U}$  and  $^{232}\text{Th}$  radioactive series and  $^{40}\text{K}$ . Minerals containing the  $^{238}\text{U}$  and  $^{232}\text{Th}$  radioactive series are highly radioactive. The concentrations of  $^{238}\text{U}$ ,  $^{232}\text{Th}$  and  $^{40}\text{K}$  depend on the type of rock from which the soils originate. Higher radiation levels are found in igneous rocks, such as granite, while lower levels in sedimentary rocks [1].

The thorium-to-uranium ratio is a geochemical tool used in various fields of science, such as geology, geochemistry, and archaeology. It represents the relative abundance of thorium (Th) and uranium (U) isotopes in a sample. The Th/U ratio helps differentiate between magmatic rocks formed from different sources. Igneous rocks typically have Th/U ratios ranging from 2.5 to 7.0. Deviations from this range can indicate specific magma sources or processes involved in rock formation. The Th/U ratio in sedimentary rocks can provide insights into the oxygen levels (redox conditions) present during their deposition. Low Th/U ratios (<2) generally indicate anoxic environments, while higher ratios suggest toxic conditions. This information helps reconstruct the paleoclimate and understand the evolution of sedimentary basins [2].

The Th/U ratio in zircon crystals can be used to determine their origin and age. Zircon crystals with high Th/U ratios are more likely to be of magmatic origin [3], while those with low ratios are more likely to be

metamorphic. This information is crucial for understanding the geological history of a region [4].

Investigation of Th/U ratio is necessary to perform a quantitative analysis of uranium. This ratio indicates the extremely specific regimes of the rock formation where uranium is characterized by both toxicity and chemical toxicity, whereas thorium is to be considered as only radiotoxic [5, 6]. Previous works have been conducted on igneous, sedimentary and sediment rocks to evaluate their chemical composition, Th/U ratio and age [7-9].

Different techniques have been used to determine the uranium and thorium concentrations in naturally occurring radioactive materials (NORM), such as alpha-particles spectrometry with semiconductor detectors, inductively coupled plasma mass spectroscopy (ICP-MS), neutron activation analysis, liquid scintillation counting and gamma-ray spectrometry. These techniques are very expensive.

Solid state nuclear track detectors (SSNTDs) are widely used as an effective tool to measure alpha tracks emitted from radioactive material [10]. It is a simple, inexpensive, and non-destructive technique. Since their discovery, (SSNTDs) have been used in almost all branches of science and technology. It is become an important tool in investigation of the presence of radon gas, not only in indoor air but also in the soil. SSNTDs are also used to determine the uranium and thorium contents in geological samples [11].

The present work focuses on applying the SSNTD methodology as an alternative, relatively sensitive

---

\* [hsamman@acuegypt.edu](mailto:hsamman@acuegypt.edu)

radiometric technique with a low per sample cost to evaluate the  $^{232}\text{Th}$  to  $^{238}\text{U}$  ratio in NORM samples and compare the obtained Th/U values to those resulting from gamma-ray and mass spectrometry techniques.

## 2. EXPERIMENTAL AND ANALYTICAL TECHNIQUES

### 2.1. Samples collections

Twenty-one samples were collected, 10 cm from the surface, from four different locations in Eastern deserts in Egypt. These samples were grouped into three groups; first group contained natural rock samples rich in U, the second group natural rock samples rich in Th, while the third group contained natural rock samples with different concentrations of both U and Th.

### 2.2. Gamma-ray spectrometry

The collected samples were dried at 105 °C for 24 hours to eliminate the moisture content. The samples were crushed and sieved through 200 mesh size (74 microns). The samples were weighed and placed in polyethylene beakers of 250 cm<sup>3</sup>. The beakers were completely sealed for one month to allow secular equilibrium between  $^{222}\text{Rn}$  and its daughters.

Gamma-ray spectrometer used in this study consists of 100% relative efficiency n-type hyper pure germanium detector (HPGe) connected to X-cooler-III electric cooling system. The X-cooler cooling system is used to assure permanent cooling of the detector. The detector is surrounded by reprocessed high-performance and low-background lead shield cylinder 10 cm thick. A graded liner of copper and tin layers is provided for the suppression of lead X-rays. The detection range is between 10 keV and 10 MeV. The detector has a resolution (FWHM) of 1.9 keV at 1332 keV. The detector is connected to a digital spectrometer DSPC-pro which includes high voltage, advanced spectroscopy amplifier and 16 k multichannel analyzer. The acquisition system and analysis of spectra are controlled by gammaVision software [12]. The energy and efficiency calibration were performed using multi-gamma standard reference source [13]. Angle-3 software was used to generate efficiency curves considering the volume of the sample and density.

The sample container was placed on the top of the detector for counting. The high-activity samples were counted over a period of 6 hours (live time) while the low-activity samples were counted for 24 hours live time. The analysis of the collected samples has been carried out using GammaVision software [12]. The spectra have been corrected for background self-absorption, density which ranged between 0.6 and 2.6 g.cm<sup>3</sup> [14] which depends on the density of the sample [15, 16].

The specific activity of  $^{238}\text{U}$  was determined from gamma line 1001 keV. The specific activity of  $^{232}\text{Th}$  was determined from 911.07 and 2614.47 keV gamma photons emitted from  $^{228}\text{Ac}$  and  $^{208}\text{Tl}$  daughters, respectively (average value) since  $^{232}\text{Th}$  does have well defined gamma photon and the  $^{40}\text{K}$  was determined

from its gamma-ray energy peak of 1460.83 keV. The nuclide activity in Bq.kg<sup>-1</sup>, based on the peak at energy E, was calculated using equation [12]:

$$A_{Ei} = \frac{N_{Ei} * DTC * RSF * GeoFac * Ac}{LT * \epsilon_E * B_r * DIV * s} \quad (1)$$

where:  $N_{Ei}$  is net counts area for peak at energy E, DTC decay corrections, RSF random summing correction factor, LT live time,  $\epsilon_E$  detector efficiency at energy E,  $B_r$  peak branching ratio from library, GeoFac geometry correction factor, Ac attenuation correction, DIV divisor reported in the nuclide peak matrix (if requested), and s is the sample mass in kilograms.

The final activity of the nuclide is the average of the peak activity of the qualifying peaks defined in the library. The minimum detectable activity estimated from count rate ( $CR_{mda}$ ) using the Traditional ORTEC method as given by equation:

$$CR_{mda} = \frac{\frac{100}{SENS} \left\{ \sqrt{2 * B_1 + \frac{2500}{SENS^2}} + \frac{50}{SENS} \right\}}{LT} \quad (2)$$

where: SENS is Peak Cut off value (%), LT live time (in seconds), and  $B_1$  is the background term.

The minimum detectable activity was found to be 3.49, 62.78 Bq.kg<sup>-1</sup> and 19.30 Bq.kg<sup>-1</sup> for  $^{232}\text{Th}$ ,  $^{238}\text{U}$  and  $^{40}\text{K}$ , respectively.

### 2.3. Solid-state nuclear track detection techniques

In the present work a new method is proposed to form a thin source from the rock sample to avoid the self-absorption of alpha emitting radionuclides.

#### 2.3.1. Forming thin layer samples

The rock samples were crushed and grinded to a very fine grain size (powder). A double side adhesive tape was fixed on a glass plate (slice). A very thin layer of rock sample powder particulates stuck on the upper side of the adhesive tape forming a thin layer of sample powder (alpha source).

The quality of the prepared thin source had been tested using an alpha spectrometer with surface barrier detector. Figure 1 shows a typical alpha spectrum collected from a rock source in a separate experiment. This spectrum sounds as if it was emitted from a thin alpha source where alpha particles peaks are well displayed with supports the applicability of the proposed method to minimize self-absorption of alpha particles in the sample.

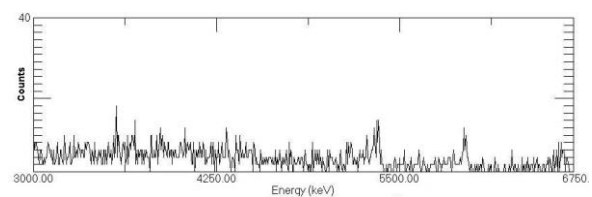


Figure 1. A typical alpha particles spectrum obtained from the thin source using a surface barrier detector.

### 2.3.2. Solid-state nuclear track measurements

Sheets of CR-39 1 cm x 1 cm 0.1 cm thick and Kodak LR-115-II cellulose nitrate film 1.5 cm x 1.5 cm 12  $\mu$ m thick were simultaneously placed in close contact to the thin layer of the rock sample powder. The detectors exposed to alpha particles emitted from  $^{232}\text{Th}$  and  $^{238}\text{U}$  during a period varied between 2 to 21 days depending on the activity of each sample. At the end of the irradiation time, the exposed detectors were etched in NaOH solution. Appropriate etching conditions of concentration, temperature and time were (2.5 N and 60 °C for 75 min in case of LR-115-II films and 6.25 N, at 70 °C for 6 hours in case of CR-39 sheets) [17, 18]. At the end of the etching time, the CR-39 and or LR-115-II sheets were washed in running water and dried at room temperature in a laboratory atmosphere. A virgin film was etched to be used for background subtraction.

The track densities for CR-39 were determined using an optical microscope with magnification (40x10) coupled with a digital camera connected to a personal computer to facilitate the examination of the alpha tracks on the computer monitor. The track density on the LR-115-II residual films was determined using a spark counter [19]. To enlarge the sizes of the track holes, “pre-sparking” was performed at 900 volts. The pre-sparked film was counted using the optical microscope where the registered alpha track appears as a bright track hole on a red background film. The average track density in each case was taken over 50 measured fields.

The track density induced (in CR-39 and/or LR-115-II) is due to the interaction of the emitted alpha particles from  $^{238}\text{U}$  (8 alphas) and/or  $^{232}\text{Th}$  (6 alphas) [20]. The track densities are proportional to the concentration of  $^{238}\text{U}$  and/or  $^{232}\text{Th}$ , respectively as given by equations [21]:

$$\begin{aligned} \rho_U^{CR} &= K_U C_U \quad \text{and} \quad \rho_{Th}^{CR} = K_{Th} C_{Th} \\ \rho_U^{LR} &= K_U C_U \quad \text{and} \quad \rho_{Th}^{LR} = K_{Th} C_{Th} \end{aligned} \quad (3)$$

where  $\rho^{CR}$  and  $\rho^{LR}$  are the track densities induced in CR-39 and/or LR-115 by alpha particles emitted from U and/or Th,  $K_U$  and  $K_{Th}$  are the detection efficiencies for U and Th, respectively.  $C_U$  and  $C_{Th}$  are the concentrations of uranium and thorium in the sample, respectively. Using the thin source approach,  $K_U$  and  $K_{Th}$  can be calculated as given by equation:

$$\begin{aligned} K_U &= \sum_{i=1}^{i=8} (1 - \sin \theta_{ci}) \quad \text{and} \\ K_{Th} &= \sum_{i=1}^{i=6} (1 - \sin \theta_{ci}) \end{aligned} \quad (4)$$

where  $\theta_{ci}$  is the critical angle of etching. For CR-39 and LR-115 the etching angle is taken to be 20° and 50°, respectively [20]. The total track density induced in CR-39 by alpha particles from U and Th is given by equation:

$$\rho^{CR} = K_U C_U + K_{Th} C_{Th} \quad (5)$$

The registration of the alpha particle track in LR-115 is limited by an energy window  $1.16 < \Delta E < 4.17 \text{ MeV}$  [20]. However, the CR-39 registers the track of all alpha

particles that hit its surface with an angle greater than the critical angle.

Based on this approach, LR-115-II registers only 4 alpha particles that have energies less than 4.5 MeV and the detection efficiency is given by equation:

$$\rho_t^{LR} = \sum_{i=1}^{i=4} (1 - \sin \theta_{ci}) C_U \quad (6)$$

Using equations (5 and 6),  $^{238}\text{U}$  and  $^{232}\text{Th}$  concentrations can be evaluated.

### 2.4. Inductively coupled plasma mass spectrometry

Samples with i) very low Th concentration and high U contained, ii) Th contained higher than U contained and iii) comparable concentration of Th and U, were measured using the ICP-MS spectrometer which classified as one of the most advanced and accurate techniques used in the field of elementary analysis. In this study, an Agilent Technologies ICP-MS (7700 Series) was used to determine the U and Th contents in some of our samples and calculate Th/U ratio.

Complete digestion of 0.5 g of each rock sample was done using a microwave digestion system (MARS6) using a mixture of 10 ml of hydrogen-fluoride HF and 10 ml of 65% concentrated nitric  $\text{HNO}_3$  acids during 30 min. To ensure complete digestion of the samples, the solutions were heated in a water bath, filtered and brought up to a volume of 50 ml using ultra-pure water. The ICP-MS detection limit for U and Th was 0.010 ppm. The ICP-MS instrument was pre-calibrated using mathematical algorithm software.

## 3. RESULTS AND DISCUSSION

### 3.1. Gamma-ray spectrometry results

The activity concentrations of  $^{238}\text{U}$ ,  $^{232}\text{Th}$  and  $^{40}\text{K}$  in the twenty-one collected samples obtained by HPGe detector is presented in Table 1. The activity concentration of  $^{238}\text{U}$  ranged from  $230.91 \pm 22.63 \text{ Bq.kg}^{-1}$  to  $100.64 \pm 1.09 \text{ kBq.kg}^{-1}$ , while the ranges of  $^{232}\text{Th}$  are from  $10.33 \pm 0.85 \text{ Bq.kg}^{-1}$  to  $115.23 \pm 0.20 \text{ kBq.kg}^{-1}$ , and  $^{40}\text{K}$  ranged from  $100.15 \pm 4.38 \text{ Bq.kg}^{-1}$  to  $21.73 \pm 0.92 \text{ kBq.kg}^{-1}$ , respectively. These results show that the activity concentration of naturally occurring radionuclides in the most measured samples are higher than the world average values of  $30 \text{ Bq.kg}^{-1}$ ,  $35 \text{ Bq.kg}^{-1}$  and  $400 \text{ Bq.kg}^{-1}$  for  $^{238}\text{U}$ ,  $^{232}\text{Th}$  and  $^{40}\text{K}$  in building materials, respectively [22]. The increased radioactivity concentration levels found in the igneous samples arise from altered radioactive materials trapped inside granite faults. However, the rock's mineral-bearing feldspar and mica content, or the fact that the rock is made of sandstones from granitic rocks, can account for the potassium activity concentration that is predominant in all sediment samples [23].

### 3.2. SSNTDs results

The activity concentrations in  $\text{Bq.kg}^{-1}$  for uranium and thorium measured with the gamma spectrometer

were converted into activity concentrations in parts per million using 1 ppm equals 12.35 Bq.kg<sup>-1</sup> for U and 4.1 Bq.kg<sup>-1</sup> for Th and the coefficients were compared to the activity concentration from SSNTDs (Figs. 2 and 3).

At low concentrations of U or Th in the sample (less than 100 ppm), the difference between the measured values by gamma and SSNTDs varied 20–40%. The poor statistics in alpha track counts at low activity can explain this discrepancy. At higher concentrations, the deviation varied between 10% and 20%. These data demonstrate that, in cases of high concentrations, SSNTDs perform reasonably well in determining U and/or Th concentrations. However, there are some drawbacks, such as long measurement time, the need to use an optical microscope for counting alpha tracks (unless an advanced microscope is available).

Table 1. The specific activities (Bq.kg<sup>-1</sup>) of <sup>238</sup>U, <sup>232</sup>Th and <sup>40</sup>K in all the collected samples.

	<sup>238</sup> U	<sup>232</sup> Th	<sup>40</sup> K
1	90659.54±689.14	67.26±6.92	560.33±34.83
2	4394.37±64.65	10.33±0.85	118.83±6.69
3	51838.57±571.95	58.31±7.97	334.52±32.72
4	508.42±20.03	59.46±0.73	348.02±3.75
5	565.66±21.85	47.43±0.66	293.01±3.41
6	28374.39±598.51	102.39±0.34	882.00±59.25
7	7188.75±80.85	16.35±1.36	100.15±4.38
8	7751.13±341.71	18.10±3.00	142.43±22.16
9	100641.42±1087	1842.86±44.00	21733.77±916.25
10	307.26±25.89	34.76±0.71	313.47±4.41
11	522.60±185.31	4632.68±3.86	1144.82±55.17
12	424.75±150.79	4037.15±9.56	874.94± 47.46
13	230.91±22.63	106.08±1.08	1501.88±8.23
14	2024.81±72.72	8740.40±8.37	1880.67±12.20
15	2029.91±56.85	5668.61±6.80	1724.92±10.94
16	19525.10±182.94	1753.61±6.72	2003.49±19.74
17	834.93±29.48	587.54±2.09	298.35±4.26
18	8937.98±122.57	9278.23±10.60	2052.18±18.31
19	3109.81±79.05	2152.81±5.48	673.61±9.38
20	15988.94±1105.36	115234.39±203	9582.31±175.88
21	9294.10±676.93	41878.96±97.31	3698.30±112.41

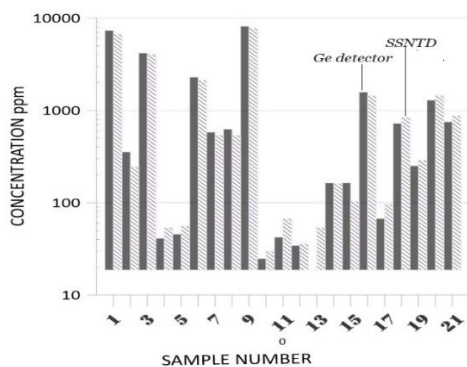


Figure 2. A comparison of U concentrations (ppm) measured by gamma spectroscopy and by SSNTDs.

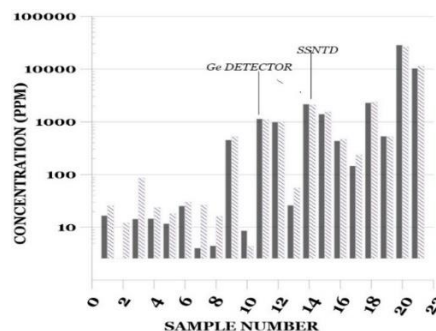


Figure 3. A comparison of Th concentrations (ppm) measured by gamma spectroscopy and SSNTDs.

### 3.3. ICP-MS results

Table 2 lists the Th/U ratio obtained using gamma spectroscopy and SSNTDs along with the resulting Th/U ratio as measured by ICP-MS for 11 samples.

The data show a good agreement between Th/U ratio as obtained by gamma spectrometer and ICP-MS at very low concentration of Th and high concentration of U (samples 1, 3, 6, and 9). Whenever the concentrations of Th and U are comparable, a good agreement between the Th/U ratio obtained by the three techniques (samples 13, 20 and 21).

There is good agreement between the Th/U ratios for samples 4, 5, 6, 9, 12, 13, 14, and 16–21 that were obtained using a gamma spectrometer and SSNTDs where maximum deviation in Th/U value was 29%. However, the obtained value of Th/U by employing SSNTDs were very far from the Th/U obtained by gamma spectroscopy for samples 1, 2, 3, 7 and 8 with very low Th concentration and high U contents.

Table 2. The concentration of Th to the concentration of U as deduced by gamma, SSNTDs and ICP-MS techniques.

Sample	Th / U		
	HPGe	SSNTDs	ICP-MS
1	0.002	0.004	0.002
2	0.007	0.050	
3	0.003	0.021	0.003
4	0.359	0.445	
5	0.257	0.326	
6	0.011	0.014	0.009
7	0.007	0.050	
8	0.007	0.030	
9	0.056	0.068	0.0471
10	0.347	0.148	
11	27.209	16.448	
12	29.173	28.302	10.533
13	1.410	1.037	1.147
14	13.249	13.129	7.363
15	8.571	15.047	
16	0.276	0.326	1.783
17	2.160	2.460	
18	3.186	2.839	1.819
19	2.125	1.828	
20	22.121	18.424	18.436
21	13.830	12.892	11.77

The high values of Th/U ratio in some samples are an indication that the rock is thorium rich or uranium deficient. This is due to natural processes [23] such as

weathering and leaching, where migration or accumulation of uranium may be taking place. It provides an indication whether relative depletion of U or initially poor U source (Clark value greater than 3.5) or enrichment of U had occurred [23]. The variation of Th/U ratios in the same rock type is mainly due to source heterogeneities and uranium mobilization processes. Large Th/U ratio variation can be explained by sample composition, fractional crystallization, and U mobilization [24].

Figure 4 illustrates a comparison between Th/U ratio as measured by gamma, ICP-MS spectroscopy and SSNTDs. By comparing Table 2 and (Figure 4), a good agreement among the Th/U ratios obtained by the three techniques in samples 6, 12, 13, 14, 18, 20 and 21 and a fair agreement between the obtained ratio values in samples 1, 3, 9 and 16.

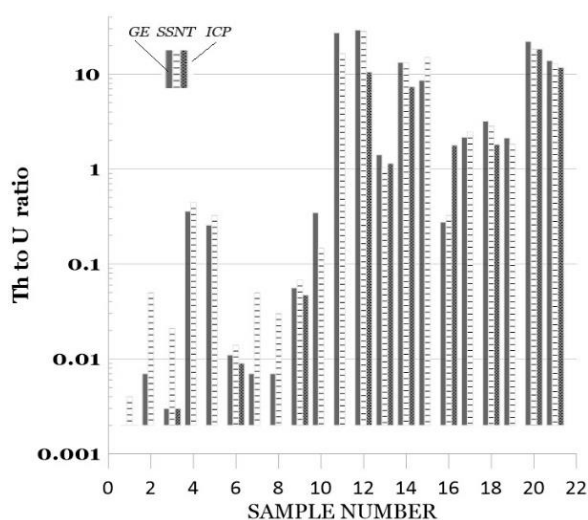


Figure 4. Th/U ratios measured by gamma spectrometry, SSNTDs and ICP-MS.

#### 4. CONCLUSION

For the purposes of the CR-39 and LR-115 alpha tracks applications, a novel technique for creating a thin alpha source from rock samples is presented and tested by using alpha particles spectrometer. Th and U concentrations in ppm were measured in 21 NORM samples using SSNTDs, and the results were compared to those obtained by gamma and ICP-MS spectrometers. The obtained Th/U ratio varied from 0.002 to 22 depending on rock type. For most of the rock samples, the measurements yield Th/U ratio values that are in relatively good agreement. For most of the samples, the maximum deviation in Th/U ratio determined using gamma spectrometer and SSNTDs is 29%.

**Acknowledgements:** The authors would like to thank Dr. Ahmed Abdelgawad, Faculty of science Cairo University, for his help and offering ICP-MS.

#### REFERENCES

1. A. Olanya, D. Okello, B. Oruru, A. Kisolo, "The Primordial Radionuclides Activity Concentrations and Associated Minerals in Rocks from Selected Quarries in Northern Uganda," *IJSBAR*, vol. 66, no. 1, pp. 45 – 65, Dec. 2022. Retrieved from: <https://core.ac.uk/download/552586824.pdf> Retrieved on: Sep. 22, 2023
2. L. Cao et al., "Discussion on the applicability of Th/U ratio for evaluating the paleoredox conditions of lacustrine basins," *Int. J. Coal Geol.*, vol. 248, no.1, 103868, Dec. 2021. DOI: 10.1016/j.coal.2021.103868
3. C. L. Kirkland, R. H. Smithies, R. J. M. Taylor, N. Evans, B. McDonald, "Zircon Th/U ratios in magmatic environs," *Lithos*, vol. 212 – 215, pp. 397 – 414, Jan. 2015. DOI: 10.1016/j.lithos.2014.11.021
4. C. Yakymchuk, C. L. Kirkland, C. Clark, "Th/U ratios in metamorphic zircon," *J. Metamorph. Geol.*, vol. 36, no. 6, pp. 715 – 737, Aug. 2018. DOI: 10.1111/jmg.12307
5. L. P. Rikhvanov, "Using Radioactive Elements and the Th/U Ratio in Study of the Geochemical Typification of Granitoids and Their Intrusive Character," *Russ. Geol. Geophys.*, vol. 60, no. 9, pp. 1018 – 1025, Sep. 2019. DOI: 10.15372/RGG2019067
6. A. G. Doroshkevich, D. A. Chebotarev, V. V. Sharygin, I. R. Prokopyev, A. M. Nikolenko, "Petrology of alkaline silicate rocks and carbonatites of the Chuktukon massif, Chadobets upland Russia: Sources, evolution and relation to the Triassic Siberian LIP," *Lithos*, vol. 332 – 333, pp. 245 – 260, May 2019. DOI: 10.1016/j.lithos.2019.03.006
7. B. M. Al-Zahrani, H. S. Alqannas, S. H. Hamidalddin, "Study and Simulated the Natural Radioactivity (NORM) U-238, Th-232 and K-40 of Igneous and Sedimentary Rocks of Al-Atawilah (Al-Baha) in Saudi Arabia," *WJNST*, vol. 10, no. 4, pp. 171 – 181, Oct. 2020. DOI: 10.4236/wjnst.2020.104015
8. M. M. El Galy, A. M. El Mezayn, A. F. Said, A. A. El Mowafy, M. S. Mohamed, "Distribution and environmental impacts of some radionuclides in sedimentary rocks at Wadi Naseib area, southwest Sinai, Egypt," *J. Environ. Radioact.*, vol. 99, no. 7, pp. 1075 – 1082, Jul. 2008. DOI: 10.1016/j.jenvrad.2007.12.012
9. J. D. DePaolo, V. E. Lee, J. N. Christensen, K. Maher, "Uranium comminution ages: Sediment transport and deposition time scales," *C. R. Geosci.*, vol. 344, no. 11 – 12, pp. 678 – 687, Nov. 2012. DOI: 10.1016/j.crte.2012.10.014
10. T. A. Salama, U. Seddik, T. M. Dsooky, A. A. Morsy, R. El-Asser, "Determination of thorium and uranium contents in soil samples using SSNTD's passive method," *PRAMANA*, vol. 67, no. 2, pp. 269 – 276, Aug. 2006. DOI: 10.1007/s12043-006-0071-4
11. L. Oufni, M. A. Misdaq, "Radon emanation in a limestone cave using CR-39 and LR-115 solid state nuclear track detectors," *J. Radioanal. Nucl. Chem.*, vol. 250, no. 2, pp. 309 – 313, Nov. 2001. DOI: 10.1023/A:1017951713943
12. *GammaVision Analysis version 8*, ORTEC, Oak Ridge (TN), USA, 2015.
13. *Standard reference source number 122162B*, Eckert & Ziegler Analysis, product code:8503-EG-SD, Jan. 2022.
14. M. O. Miller, "Modeling a HPGe detector's absolute efficiency as a function of gamma energy and soil density in uncontaminated soil," *SDRP J. Earth Sci. Environ. Stud.*, vol. 3, no. 4, Dec. 2018. DOI: 10.25177/JESES.3.4.2. 2018

15. N. Q. Huy, T. V. Luyen, “A method to determine  $^{238}\text{U}$  activity in environmental soil samples by using 63.3-keV-photopeak-gamma HPGe spectrometer,” *Appl. Radiat. Isot.*, vol. 61, no. 6, pp. 1419 – 1424, Dec. 2004.  
DOI: 10.1016/j.apradiso.2004.04.016
16. J. Al-Tuweity, H. Kamleh, M. S. Al-Masri, A. W. Doubal, El M. Chakir, “Self-absorption correction factors: Applying a simplified method to analysis of Lead-210 in different environment samples by direct counting of low-energy using HPGe Detector,” *E3S Web Conf.*, vol. 240, 03002, 2021.  
DOI: 10.1051/e3sconf/202124003002
17. A. K. Mheemeed, A. Kh. Hussein, R. B. Alkhayat, “Characterization of alpha-particle tracks in cellulose nitrate LR-115 detectors at various incident energies and angles,” *Appl. Radiat. Isotopes*, vol. 79, pp. 48 – 55, Sep. 2013.  
DOI: 10.1016/j.apradiso.2013.04.020
18. M. D. Salim, A. A. Ridha, N. F. Kadhim, A. El- Taher, “Effects of Changing the Exposure Time of CR-39 Detector to Alpha Particles on Etching Conditions,” *J. Rad. Nucl. Appl.*, vol. 5, no. 2, pp. 119 – 125, May 2020.  
DOI: 10.18576/jrna/050206
19. D. Stanić, M. P. Sovilj, I. Miklavčić, V. Radolić, “Determination of track counting loss threshold of spark counter due to high track densities on strippable LR115 II nuclear track detectors,” *Radiat. Meas.*, vol. 106, pp. 591 – 594, Nov. 2017.  
DOI: 10.1016/j.radmeas.2017.03.035
20. A. F. Hafez “A new method for determining uranium and thorium,” *Nucl. Instr. Methods Phys. Res.*, vol. 69, pp. 373 – 381, 1992.
21. S. A. Eman, S. H. Nageeb, A. R. El-Sersy, “U and Th Determination in Natural Samples Using CR-39 and LR-115 Track Detector,” *WJNST*, vol. 2, no. 1, pp. 36 – 40, Jan. 2012.  
DOI: 10.4236/wjnst.2012.21006
22. M. Charles, “UNSCEAR Report 2000: Sources and Effects of Ionizing Radiation,” *J. Radiol. Prot.*, vol. 21, no. 1, pp. 83 – 86, Mar. 2001.  
DOI: 10.1088/0952-4746/21/1/609
23. N. K. Ahmed, A. G. M. El-Arabi, “Natural radioactivity in farm soil and phosphate fertilizer and its environmental implications in Qena governorate, upper Egypt,” *J. Environ. Radioact.*, vol. 84, no. 1, pp. 51 – 64, 2005.  
DOI: 10.1016/j.jenvrad.2005.04.007
24. M. Tzortzis, H. Tsertos, “Determination of thorium, uranium and potassium elemental concentrations in surface soils in Cyprus,” *J. Environ. Radioact.*, vol. 77, no. 3, pp. 325 – 338, 2004.  
DOI: 10.1016/j.jenvrad.2004.03.014